UNIVERSITAT POLITÈCNICA DE CATALUNYA


# Investigation on Corrosion Protection applying organic–inorganic sol–gel coatings on AA2024-T3

## Corrosion Aluminium Protection

**Caroline Velasques Ugarteche**

**28/06/2013**

**Advisor:** Prof. Dr. Elaine Armelin

# 1. Table of contents

## 2. Abstract

In order to prevent corrosion on aluminium and aluminium alloys, many surface treatments have been developed, such as silane films, which are environmentally compliant coatings. During this work we investigate corrosive behaviour of aluminum alloys AA2024 in a NaCl 0.05mol $L^{-1}$ coated with MEMO/Bis-EGMP/TiB, during the Part A and TEOS/ATMP/GPTMS during the Part B.

The aluminium alloy substrates were pre-threated before the coating deposition. The silane coatings were applied using sol-gel system. After silane curing process, all the substrates were covered with a commercial epoxy coating in order to provide the topcoat protection before the samples immersion in the aggressive solution for corrosion tests (NaCl 3.5%).

Electrochemical techniques were applied during Part A in order to evaluate the corrosion protection of silane coating. Microscope and optical analysis was carried on during this work to evaluate the film surface homogeneity and the presence or absence of defects. The samples prepared were tested under accelerated corrosion environment, which showed that the samples prepared on Part A of the present study did not have good protection performance. On the other hand, samples prepared during Part B showed excellent behaviour and the silane coating prepared from TEOS/ATMP/GPTMS system protected the aluminium surface from the aggressive corrosion medium. Adherence of silane system and also the topcoat applied is essential to obtain a long time protection. Therefore, pull-off tests were performed to confirm the efficacy of the coating adherence.

# 3. Objectives

This investigation was divided in two parts. The objective of Part A was to study the effect of TiB (Titanium(IV) butoxide) as catalyst on the sol-gel preparation of Bis-EGMP (Bis- 2-(methacry-loyloxy)ethyl phosphate) and MEMO ([3-(Methacryloyloxy)propyl]trimethoxysilane) system. During the part B the objective was to continue with past investigations with the use of inhibitors based on TEOS/ATMP/GPTMS (tetraethylorthosilicate / aminotrimethylenephosphonic acid / glycidoxypropyltrimethoxysilane) silane coatings.

On the first part the mainly objective is to evaluate the incorporation of phosphorus components in silane hybrid films formation, accelerating the curing process with a catalyst promoter. Kannan et. al have studied the copolymerization of EGPM (2-(methacryloyloxy)ethyl phosphate) with MEMO (Kannan, Choudhury and Dutta, 2007). They were able to form a Si-O-P network with high thermal stability. These materials were selected because they have a combination of three different groups: Methacryloxy, phosphate and silicon-alcoxy groups. During this research non-coated aluminium and coated aluminium corrosion resistance were compared. Bis-EGMP was chosen because it has one more phosphorus group than Kannan et. al. work, which we suppose it would make easier the formation of Si-O-P network. TiB was selected as catalyst material because it is able to form Si-O-Ti and P-O-Ti linkages that turn the film formation into a more stable coating.

During the second part of the investigation, corrosion tests were carried on in order to finish previous studies made with TEOS/Phosphonic systems for silane coating adhesion. Corrosion tests using NaCl solution were performed to prove the efficacy of a bilayer coating made of silane-epoxy films prepared in previous works. Dalmoro et. al. investigated the corrosion behaviour of AA2024 coated with TEOS and ATMP system with good electrochemical results (Dalmoro, Santos and Azambuja, 2011). However, they did not test glycidoxypropyltrimethoxysilane component. Our main aim is evaluate the influence of the new three-system composition on the aluminium AA2024-T3 protection against chlorine aggressive ions.

# 4. Introduction

Aluminium is one of the most used metals and the most available one in the Earth. It is known for its excellent properties as low density, high conductivity and easy machining (Liu *et al.*, 2005). The excellent mechanical properties of aluminium 2024 alloys justify the extensive use of these alloys for several applications. Because of the presence of alloying elements, the intermetallic components precipitate. This leads to localized electrochemical activities. So, aluminium AA2024 is inclinable to develop localized corrosion (Álvarez *et al.*, 2010).

Due to its prone to pitting corrosion, it is necessary that aluminium 2024 receives a pre-treatment in order to prevent future corrosion damages and prepare the surface for painting. Currently, the conversion coating on aluminium alloy is either developed anodically by an applied electric current or developed chemically on the aluminium surface by reaction with chromium solutions (Joshua Du *et al.*, 2001). But this last system is not environmentally friendly, once chromium has high toxicity.

In order to reduce the application of chromium in this process, silane systems have been studied as alternatives for coating aluminium alloys (Álvarez *et al.*, 2010; Joshua Du *et al.*, 2001; Kannan, Choudhury and Dutta, 2007; Liu *et al.*, 2005; Wang and Bierwagen, 2009; Wittmar *et al.*, 2012; Zhang *et al.*, 2007; Zheng and Li, 2010). Silanes are cheap alternatives for the chromium system and it can also be applied on the surface using low temperatures with environmentally friendly components. Electrochemical, surface analysis and accelerated corrosion tests were made for identify the efficacy of the Bis-EGMP/MEMO/TiB coatings on AA2024 aluminium alloys on the first study and accelerated corrosion tests were carried on in order to investigate the efficacy of TEOS/inhibitor silane system.

# 5. State of the Art

## 5.1 AA2024-T3

Aluminium is spread used around the world for applications that require low density and high mechanical properties, as maritime and aeronautic applications.

Aluminium alloys from 2XXX series have Cu as second mainly element. The nominal composition of elements besides aluminium in this alloy is showed on Table 1 ( Dalmoro et. al. 2009). The code T3 indicates the thermal treatment identification for this alloy, showing that this material was treated in three steps. First step is the solution heating treatment, second is a furnace cooling and third is an artificial aging (Zhang and Frankel, 2003).

**Table 1: Nominal composition of 2024 aluminium alloy**

| Elements | Cu | Mg | Si | Fe | Mn | Cr | Zn | Ti | Other |
|---|---|---|---|---|---|---|---|---|---|
| Mass proportion | 3,8-4,9 | 1,2-1,8 | 0,5 | 0,5 | 0,3-0,9 | 0,1 | 0,15 | 0,15 | 0,15 |

Due to the non-homogenous distribution of Cu and other intermetallic along the material, it can develop micro cells for galvanic corrosion. Because of it, this alloy has weak resistance against pitting corrosion (Dalmoro, 2009).

Pit corrosion is characterized by pit formation. Pits are usually really small but under severe conditions they may perforate the material. The small micro cells formed by non-homogenous distribution are composed for two metals (Cu and Al as instance) and electrolyte, this lead to galvanic localized corrosion. The attack to less noble metal can continue until the aluminium from vicinity is completely consumed.(Dietrich G. Altenpohl, 1998) Pitting corrosion often initiates on or around the copper-rich intermetallic compound particles (the second phase particles) in Al 2024-T3. Micro flaws in the oxide film exist at the heterogeneity sites and potential differences exist between the intermetallic particles and the Al matrix. These micro-flaws and the galvanic couples would

result in localized attack and enhance the susceptibility of Al 2024-T3 to pitting corrosion when the alloy is exposed to solutions containing chloride ions. (Shao *et al.*, 2003). In Figure 1 it is possible to see an example of pitting corrosion on AA2024-T3 after being exposed for 2h in NaCl 0,01M (Shao *et al.*, 2003)

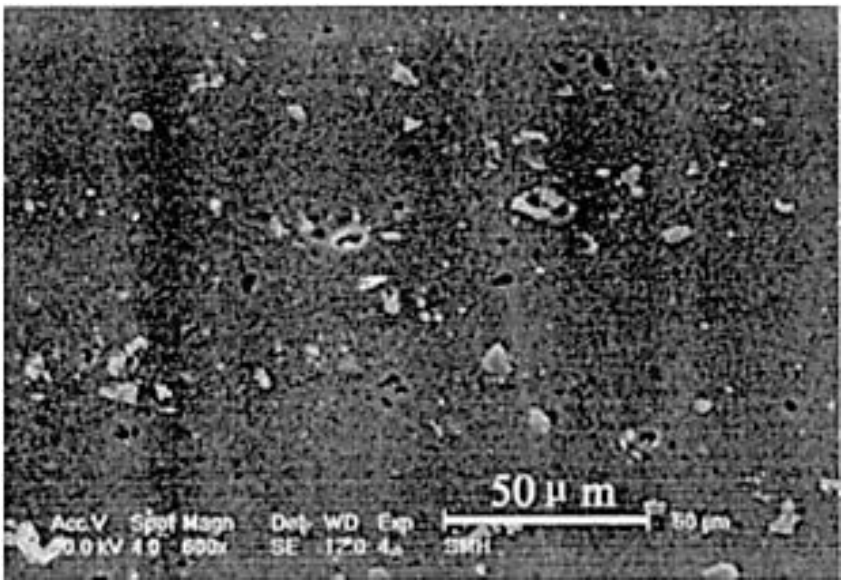


**Figure 1: Pitting corrosion on AA2024-T3 exposed for 2h under NaCl 0,01M**

The high mechanical properties in AA2024-T3 occur because of precipitation of intermetallic particles. Therefore, especially for AA2024-T3 the treatment for building up the conversion coating must be below 120ºC to prevent the deterioration of the mechanical properties because intermetallic particles dissolution. (Wittmar *et al.*, 2012). Figure 2 represents an $Al_2CuMg$ particle, one of the responsible for the high mechanical properties of AA2024-T3 (Shao *et al.*, 2003)

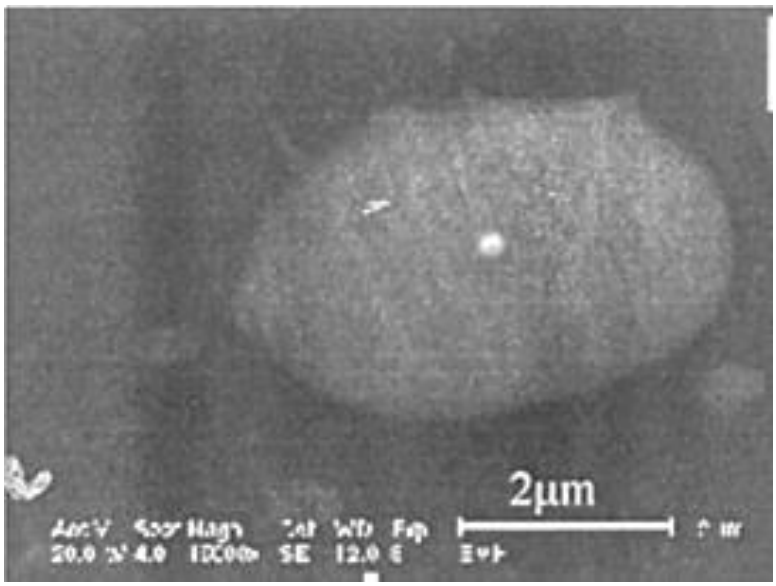


**Figure 2: SEM imaging of an intact $Al_2CuMg$ particle.**

## 5.2 Silane film

Silane is a type of polymer made of a Si and O backbone. The strong bond between these components is responsible for high thermal stability and compatibility with metal surfaces. If they are functionalized with organic components they can provide a link between the metallic surface and paints or adhesives (Wu *et al.*, 2007). When organic and inorganic components work together, they are called as hybrid silanes and this material combines properties from inorganic and organic material. The organic components are able to increase coating thickness and lower cure temperature, while the inorganic components are responsible for adhesion with the metal surface (Zheng and Li, 2010).

Silane films can be produced by sol-gel process. In this process a precursor solution get gelatinized by evaporation of the solvent, and then is cured in order to form the final net. Using this process it is not necessary to have high temperatures and it leads to homogeneous materials (Durán *et al.*, 2007).

It is possible to divide the sol-gel formation in four steps: First the precursor hydrolysis in order to form Si-OH bonds, second the condensation and polymerization of the monomers occur providing the chain formation. The third step corresponds to the particles growth. The last step is the agglomeration and formation of network (Wang and Bierwagen, 2009). The sol can be applied on the pre-treated metal surface by dip-coating and the gel formation may occur directly with solvent evaporation and post-curing thermal treatment.

## 5.3 Silane coatings applied on AA2024

In order to avoid the aluminium corrosion, a conversion coating is normally applied. Besides the well performance of chrome for building up the conversion coating, it is known that chrome is not environmentally acceptable. Because of it, many studies have been made looking for alternatives for the use of chrome (Kannan, Choudhury and Dutta, 2007; Liu *et al.*, 2005; Mrad *et al.*, 2012; Raps *et al.*, 2009; Rosero-Navarro *et al.*, 2009; Zheludkevich *et al.*, 2005, 2006).

The development of these alternatives for chromium has showed good results. Pore-free sol–gel coatings offer an effective physical barrier and also good adhesion to metal (Wittmar *et al.*, 2012).

The application of hybrid silane coatings on AA2024 forms a barrier avoiding the entrance of electrolytes and reducing the corrosion effect. Silane network has low oxygen diffusivity and the hybrid films can bond with the metal surface because of inorganic sites as well bonding with painting layers because of the organic side. In this way it is possible to make use of advantages from both inorganic and organic components. The organic constituent provides flexibility and improves compatibility with polymer coatings while the inorganic part gives superior adhesion to the metal surface and increases ductility (Raps *et al.*, 2009).

The most important for aluminium alloys is to stabilize the aluminium/sol-gel interface. The coating layer should be stable, organized and well adhered to the surface, without this layer, the corrosion protection will not be affective (Raps *et al.*, 2009).

The use of phosphorus in hybrid coating is interesting as they have important properties like increase adhesion to metals and corrosion protection. Phosphorus containing monomers are able to participate in hybrid films with other inorganic and

organic precursor. Si and P can form a Si-O-P net, resulting on a thicker and more resistant coating layer (Durán *et al.*, 2007; Kannan, Choudhury and Dutta, 2007).

To form the film on the surface the sample is submerged into the solution. SiOH groups bond with the hydroxides of the metal surface, as shown on Figure 3. After it, comes the cure process when the system will be free of water forming the chemical bond between the silane and the surface. At this point the metal surface is coated with the silane. SiOH groups that were not bonded with the metal surface can link among them; this is called the condensation step, and occurs during the hydrolysis and curing process (Dalmoro, 2009)

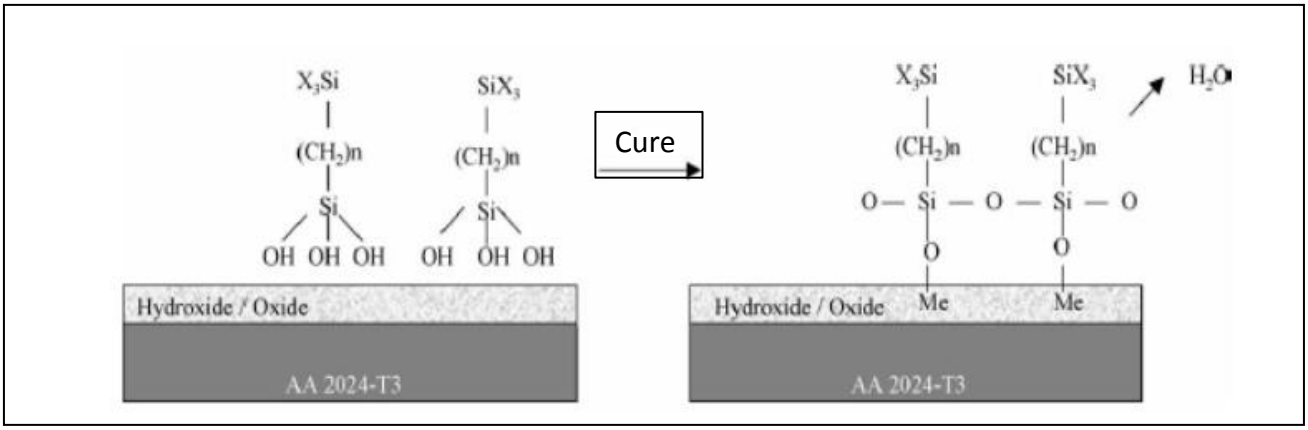


**Figure 3: Silane deposition on metallic surface**

## 5.4 Use of ATMP inhibitor on silane coatings

To be successful on avoiding the corrosion on substrate, the silane film should be completely perfect, without porous or cracks, once it works just as a barrier protector and adhesion promoter between the metal and the topcoat paint. In order to improve the protection, the use of inhibitor within the coat has been studied (Dalmoro, Santos and Azambuja, 2011; Liu *et al.*, 2013)(Natarajan, Muralidharan and Rao, 1997) Labjar *et al.*, 2010).

ATMP is considered a cheap option and acts as hydrophobic component. Phosphoric component forms a weakly soluble compound with the

metal ions, which precipitate on the surface reinforcing the protector barrier. (Natarajan et al., 1997). ATMP contains three phosphonic groups and ammonium cation, as shown in Figure 4. It has already been studied that it works as inhibitor in carbon steel acting favorably due to its good chelation properties, i.e. it can chelate with the metals cations (Labjar *et al.*, 2010; Thi Xuan Hang *et al.*, 2007).

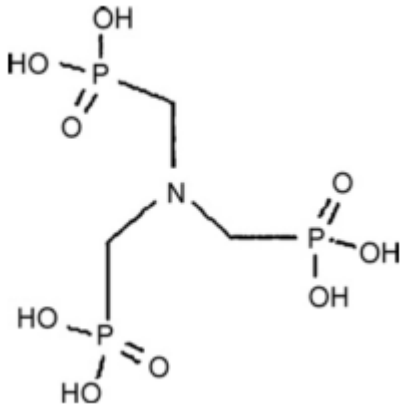


**Figure 4: Molecular structure of the aminotris-(methylenephosphonic) acid (ATMP)**

# 6. Experimental section

## 6.1 Surface preparation

Part A: Study of MEMO/Bis-EGMP/TiB system

AA2024 samples were polished using metallographic sand paper with grids 340-600-1200. After polishing, all samples were washed with distilled water, ethanol and acetone, followed by immersion during 1min in alkaline commercial cleaner (Novaclean Al 86 from Henkel company), washed with distilled water again and dried.

This process is the most important step because it prepares the surface for receiving the coating. Previous polishing guarantees that the surface will be rough to make easier the process for coating adhesion. After, cleaning with water, ethanol and acetone ensure that the surface will be degreased, and on this way the solution has directly contact with the aluminium surface. The use of Novaclean Al86 (an acid liquid commercial degreaser) performs excellently as an aluminium cleaner prior to bright dipping and anodizing operations. Its main function is to degrease and deoxidize the alloy surface. Copper, brass, magnesium, steel, titanium and other metals can also be removed and it will collaborate for bonding with phosphate molecules from the Bis-EGMP component (Kannan *et al.*, 2007). The final dry is to ensure that the substrate is free of moisture, avoiding bubbles growing during the sol-gel deposition and cure process.

Part B: Study of TEOS/ATPM/GPTMS system

The samples were prepared as described on previous studies by Dalmoro *et. al*.(Dalmoro *et al.*, 2011).

## 6.2 Coating Preparation

Part A: Study of MEMO/Bis-EGMP/TiB system

MEMO was hydrolysed in a molar proportion of 0.05/0.015/0.01 MEMO/Water/Ethanol. The hydrolysis process occurred during 6 hours, under

constantly stirring and close system to avoid ethanol evaporation. After the hydrolysis it was mixed with Bis-EGMP in a molar proportion of Bis-EGMP:MEMO by 1:1 (Kannan et. al., 2007).

This solution was divided in three parts: The first one did not receive any catalyst, on the second part 0.1% in weight of TiB was added and the last part was catalysed with 1% of TiB. All of them were diluted with 20% of ethanol, adjusting the viscosity for the coating.

The pre-treated surface samples were submerged into the solution for four minutes and slowly removed, avoiding bubbles formation and ensuring homogenously distribution. They were dried under room temperature during 24h on horizontal position for solvent evaporation. After it all samples were thermally cured under 110ºC during 3h in an oven. The cure temperature was rising slowly in order to avoid cracks on the films.

Besides the cure temperature of 110ºC, cure temperatures of 90ºC and 100ºC were also tested but the cure reaction did not occur in any of the samples. Under 110ºC, film formation was observed just on the samples prepared with TiB1%. The samples without catalyst action and with TiB0.1% did not show up any film formation, remaining a wet layer over the substrate on the first and cracked thin film on the second.

The use of temperatures over 110ºC was avoided in order to prevent degradation of mechanical properties on AA2024. As explained in previous chapters the degradation of mechanical properties for AA2024 alloys starts over 120ºC.

## Part B: Study of TEOS/ATPM/GPTMS system

The samples were prepared as described on previous studies by Dalmoro et. al..(Dalmoro et al., 2011). The proportion used for the corrosion tests was that which showed the best results of film formation on the previous work. It was demonstrated that the proportion called 3VE5, that utilizes ATMP corresponding to 46% mixture with 3% v/v of GPTMS and 1% v/v of TEOS, 50% of ethanol and concentration of ATMP was $3{,}75 \times 10^{-5}$, had best results.

Qualitative analysis was made on the samples, periodically in order to evaluate the protection and not delamination of the bilayer coating (hybrid silane-epoxy

topcoat). The samples were tested in an automatized robot simulating corrosion conditions; with cyclic test described on the 6.3.4 section.

## 6.3 Coating Characterization

### 6.3.1 Electrochemical techniques

Part A: Study of MEMO/Bis-EGMP/TiB system

Polarization curves for samples uncoated and samples coated with the solution prepared with TiB1% were measured. The tests occurred under room temperature in a solution of NaCl 0.05M, a model of the electrochemical cell is showed in Figure 5. The electrochemical cell was mounted with three electrodes. Rectangular test panels of AA2024 with 1cm$^2$ of diameter, covered with the hybrid silane cured films, were used as working electrode. As counter-electrode a stainless steel plate was used and as reference a Ag/AgCl (KCl 3M) standard electrode was employed. All the experiments were developed using AutoLab 302N potenciostate-galvanostate equipment as showed on Figure 6.

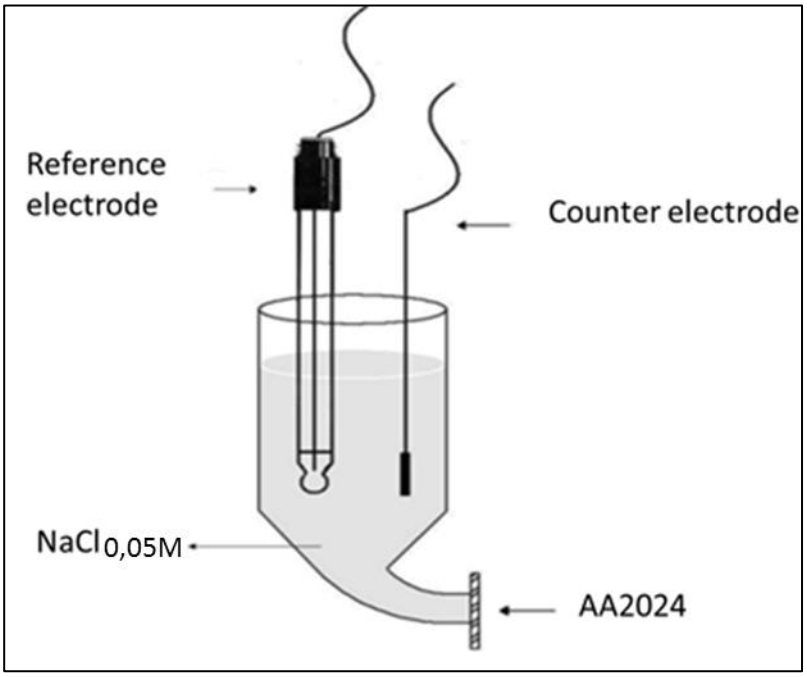


**Figure 5: Electrochemical cell used for polarization tests**

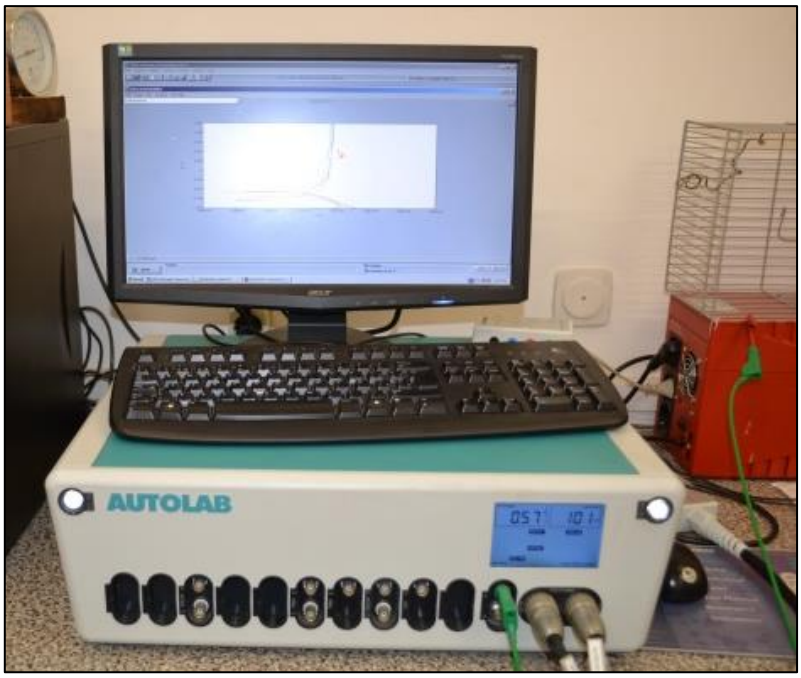


**Figure 6: AutoLab 302N potenciostate-galvanostate equipment.**

The potential was scanned from -1V to +1.25V and the response was measured on Amperes. Before starting to plot the E vs. log I curve, the work electrodes were allowed in contact with the NaCl solution for 45min in order to stabilize the system.

The polarization resistance and corrosion current were calculated using Tafel method. The corrosion currents are obtained using the polarization diagrams, as the example showed in the Figure 7 (Peres, 2010).

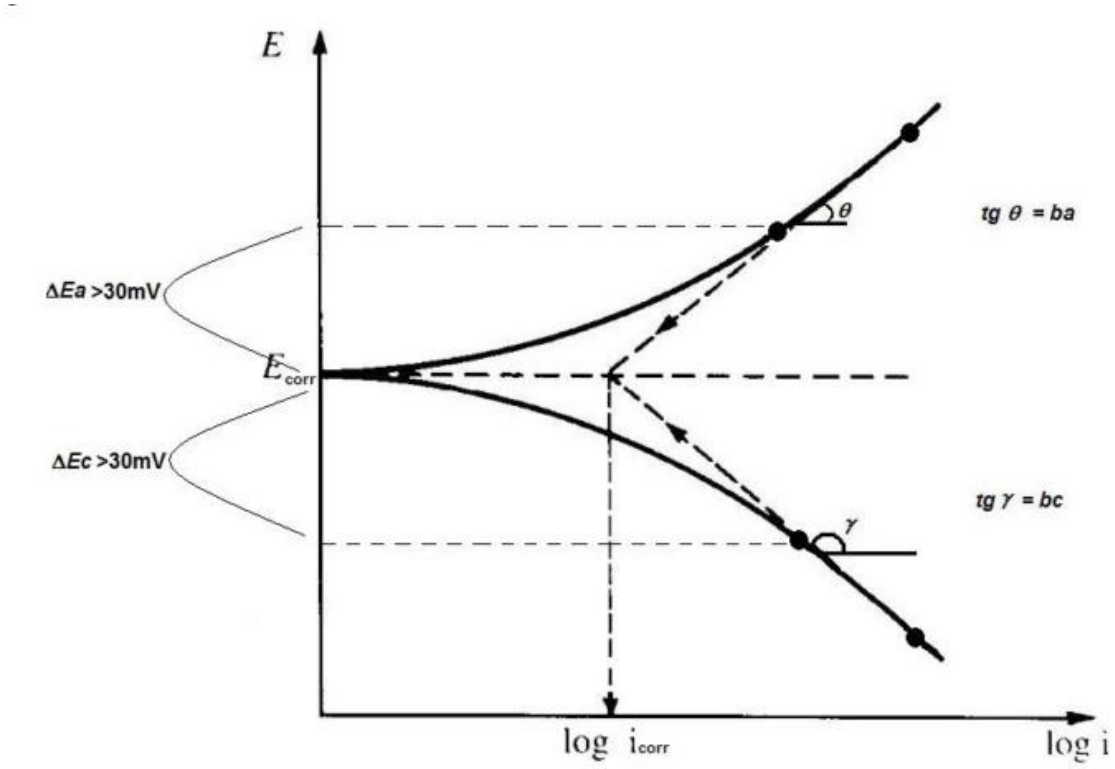


**Figure 5: Example of polarization curve and Tafel method.**

Part B: Study of TEOS/ATMP/GPTMS system

Electrochemical characterization was not performed with this system because similar studies were previously reported in Dalmoro *et al.* (Dalmoro *et al.*, 2011).

### 6.3.2 Optical microscopy

All of the samples studied on Part A and Part B were analysed on an optical microscope before being exposed to the corrosion test. Each sample were analysed weekly during the tests on this same microscope.

Using an Optical microscope it is possible to identify details until maximizing them 250x. The optical microscope used during this investigation was a Dino-Lite Optical Microscope Pro, the same model as showed on Figure 8.

**Figure 6: Dino-Lite Optical Microscope Pro, optical microscope used during this study.**

### 6.3.3 Scanning Electron Microscopy (SEM)

The surface morphology of silane films and corrosion products studied during Part A and Part B were analysed with SEM. Studies were carried out using a Focused Ion Beam Zeiss Neon40 scanning electron microscope equipped with an energy dispersive X-ray (EDX) spectroscopy system and operating at 30 kV. The equipment used is showed in Figure 9.

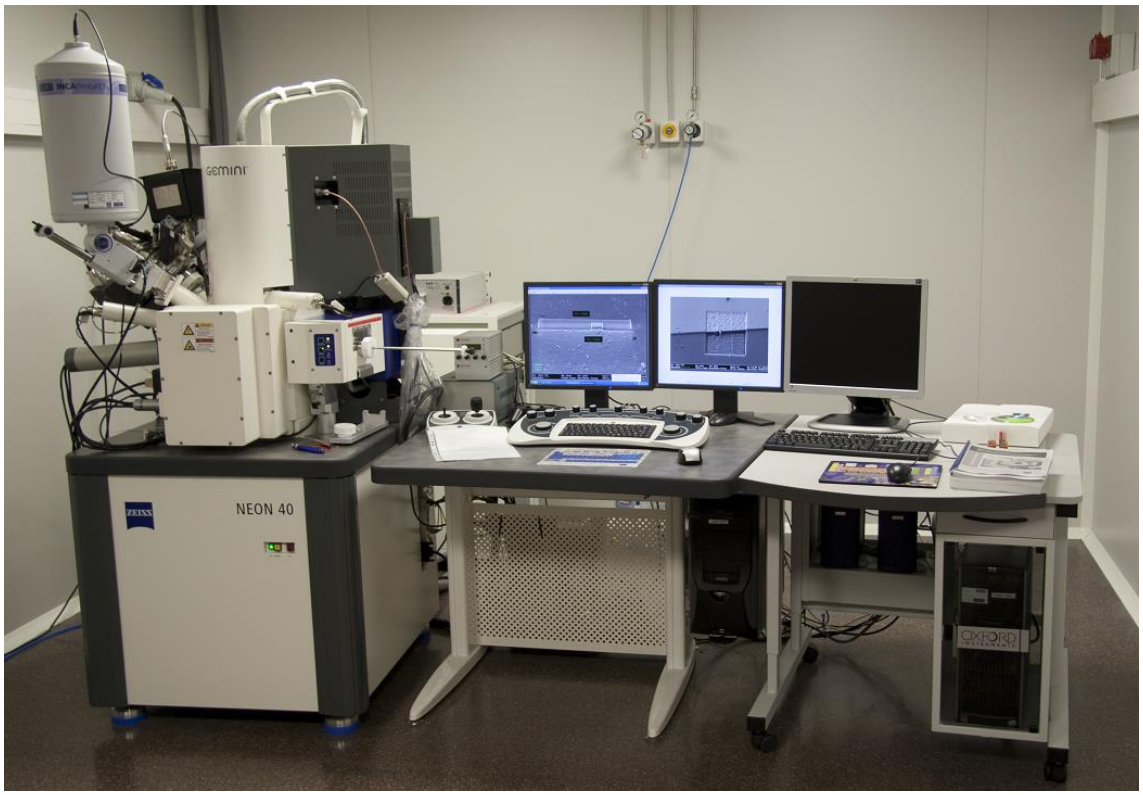


**Figure 7: Focused Ion Beam Zeiss Neon40 scanning electron microscope localized in the Center for Research in NanoEnginering (CRnE-UPC)**

### 6.3.4 Corrosion tests: Adherence and Failure area

Part A: Study of MEMO/Bis-EGMP/TiB system

For the corrosion test, samples of AA2024 were machined in a 50x50 mm shape. Two groups of samples were tested. The first group was a bilayer system, coated with the hybrid film and painted with a commercial paint explained before (epoxy topcoat). The second group was painted just with the epoxy topcoat, without silane coatings, and was called monolayer system.

The samples were qualitatively analysed after being exposed to accelerated corrosion test. An automatized programed robot for this cycle was used. It is possible to see a picture of the robot in Figure 10. It consists in two

articulated arms were the samples are localized and two 50L containers to submerge the samples.

The process consists of four steps. Once the fourth step is finish (each cycle has 60min to complete the cycle), it starts again and repeats until the samples do not resist the corrosion conditions. Details from each cycle are showed below:

1. Immersion: Samples are submerged during 15 minutes.
2. Emerging: The articulated arms emerge the samples and they are out of the water for 30 minutes.
3. Drying: 10 seconds with 60W lamps
4. Cooling: 5 minutes

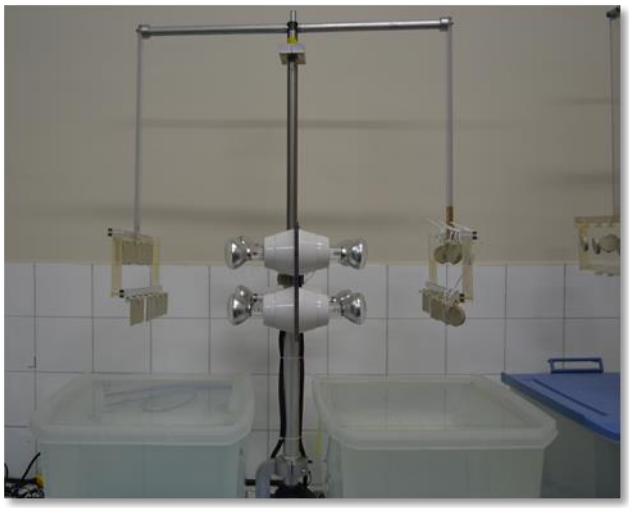

**Figure 8: Robot used for accelerated corrosion tests.**

## Part B: Study of TEOS/ATMP/GPTMS system

For the corrosion test, samples of AA2024 were machined in a 100x50 mm shape. Two groups of samples were tested. The first group was a bilayer system, coated with the hybrid film and painted with the epoxy topcoat. The second group was painted just with the epoxy topcoat, without silane coatings, and was called monolayer system. The robot used for the test was the same used for the samples studied during investigation of Part A.

The specimens studied during Part A and Part B were evaluated accordingly to the standard ASTM D1654–05. Following this standard the samples were washed with 40ºC distilled water and dried before corrosion observations. With an appropriate plain tool the rust part is scraped. After it the detached part is measured and accordingly to Table 2 it is classified.

**Table 2: Rating of creepage and failure from scribe**

| Rating Number | Creepage from Scribe (mm) | Area Failed % |
|---|---|---|
| 10 | 0 | 0 |
| 9 | De 0 a 0,5 | De 0 a 1 |
| 8 | De 0,5 a 1,0 | De 2 a 3 |
| 7 | De 1,0 a 2,0 | De 4 a 6 |
| 6 | De 2,0 a 3,0 | De 7 a 10 |
| 5 | De 3,0 a 5,0 | De 11 a 20 |
| 4 | De 5,0 a 7,0 | De 21 a 30 |
| 3 | De 7,0 a 10,0 | De 31 a 40 |
| 2 | De 10,0 a 13,0 | De 41 a 55 |
| 1 | De 13,0 a 16,0 | De 56 a 75 |
| 0 | > 16,0 | > 75 |

Accordingly to the standard ASTM D1654-05 for evaluating affected areas due to corrosion spots, all the corroded area must be unpinned from the sample surface. Using a cutter and taking care for do not damage the surface, all the surface of the sample that was affected is pulled out. A millimetre standardized paper, as showed in Figure 11, is used for calculate the affected area.

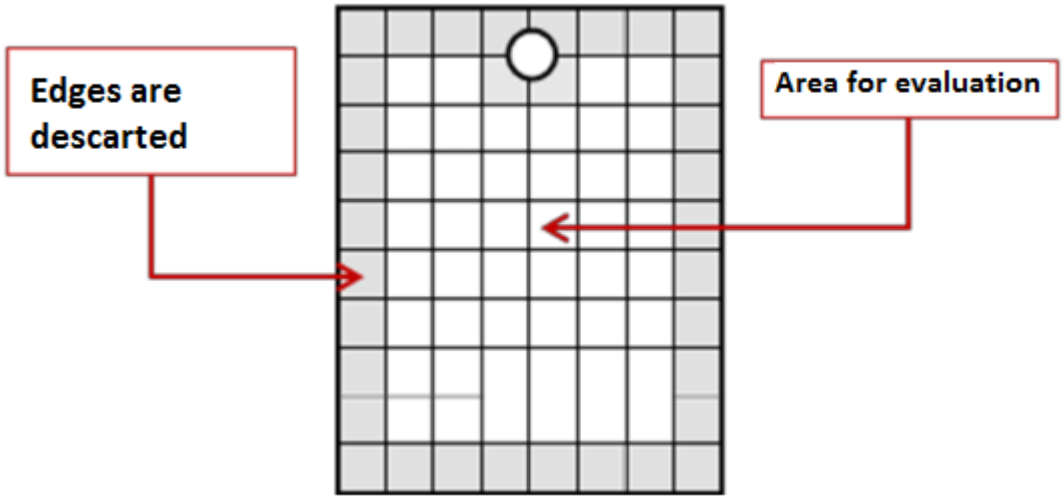


**Figure 9: Example of millimetre paper used for rating unscribed area.**

### 6.3.5 Pull-off test for adhesion measurements

The specimens were tested accordingly to ISO 4624:2002- *Paints and varnishes: Pull-off test for adhesion*. Following the standard, dollies are bonded directly to the surface of the coated material using an epoxy adhesive. After curing the adhesive, using a tensile tester, the force necessary to break the coating/substrate bond is measured.

The result of the test is the tensile stress necessary to break the weakest interface or component. The method utilized was for testing from one side only, using a single dolly, which is suitable for rigid substrates. The adhesive was curing during 24 hours, and after it the pull-off test was carried on.

The nature of the failure can also be classified. Figure 12 shows the classification for the nature of the failure.

| | |
|---|---|
| A | is cohesive failure of substrate; |
| A/B | is adhesive failure between substrate and first coat; |
| B | is cohesive failure of first coat; |
| B/C | is adhesive failure between first and second coats; |
| $n$ | is cohesive failure of the $n$th coat of a multicoat system; |
| $n/m$ | is adhesive failure between the $n$th coat and the $m$th coat of a multicoat system; |
| $-/$Y | is adhesive failure between final coat and adhesive; |
| Y | is cohesive failure of adhesive; |
| Y/Z | is adhesive failure between adhesive and dolly. |

**Figure 10: Pull-off test classification depending on the nature of failure.**

The breaking strength σ, in megapascals, for each test is given by the equation σ = F/A, where F is the breaking force in newtons and A is the area of the dolly in square millimetres.

### 6.3.6 Infrared spectroscopy (FTIR)

Tests were recorded on a FTIR 4100 Jasco spectrometer with a resolution of 4 $cm^{-1}$ in the transmittance mode and with a wavenumber range of 4000-600 $cm^{-1}$. Samples were placed directly in an attenuated total reflection accessory with a diamond crystal (Specac model MKII Golden Gate Heated Single Reflection Diamond ATR). The equipment is showed on Figure 13.

**Figure 11: FTIR spectrophotometer with ATR accessory.**

The analysis has no applicable result. The spectrums obtained did not show any conclusive result, probably the samples do not have any organic and the spectrums showed a lot of noise on background.

# 7. Results and Discussion

## 7.1 Part A: Study of MEMO/Bis-EGMP/TiB system

### 7.1.1 Electrochemical characterization

Polarization curves of samples coated and uncoated with silane system were compared. In Figure 14, is possible to compare the curves for AA2024 coated with MEMO/Bis-EGMP-TiB1% and uncoated AA2024.

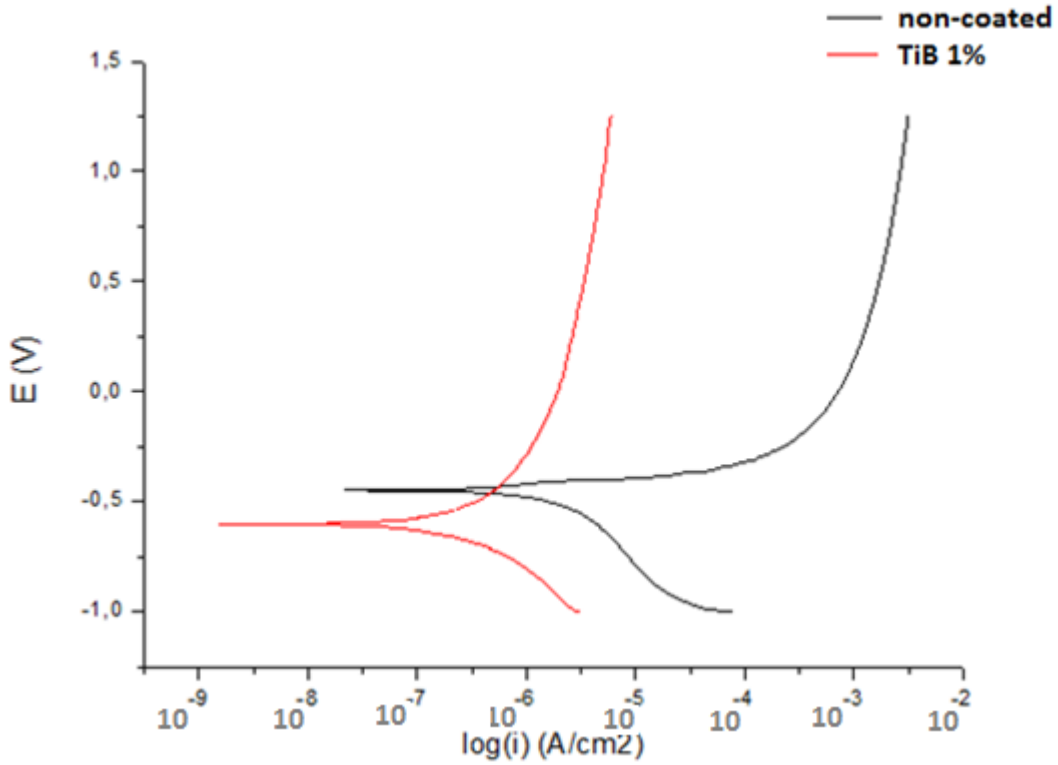


**Figure 12: Polarization curves of AA2024 in NaCl 0.05M for coated (TiB1%) and non-coated samples.**

Observing the Figure 14 it is possible to see that the sample coated with the silane had less current density response when applying voltage than

the uncoated sample. This implies that the silane coating was effective in protecting the surface of corrosion, decreasing the electron flux through the surface.

Using the data on Figure 14 and applying Tafel method, it was possible to calculate the corrosion potential, the polarization resistance and corrosion rate for the samples, as showed on Table 3.

**Table 3: Parameters obtained from Tafel method for coated and uncoated samples.**

| | Coated sample | Uncoated sample |
|---|---|---|
| Ecorr (V) | - 0,602 | - 0,443 |
| Rp (Ohm) | 6,86E+03 | 4,83E+03 |
| Corrosion rate (mm/year) | 5,36E-04 | 3,78E-03 |

Observing the parameters on Table 3 it is possible to notice that the coated sample has better polarization resistance leading to a slowly corrosion rate for this sample.

The sample coated with TiB 0.1% was also tested and did not show up any difference from the uncoated sample. As showed in Figure 15, the polarization curves for the material coated with the solution catalysed with TiB 0.1% and uncoated sample are almost the same. This probably happens because the film was cracked and did not offer barrier protection to the aluminium surface, as we observed by optical micrograph.

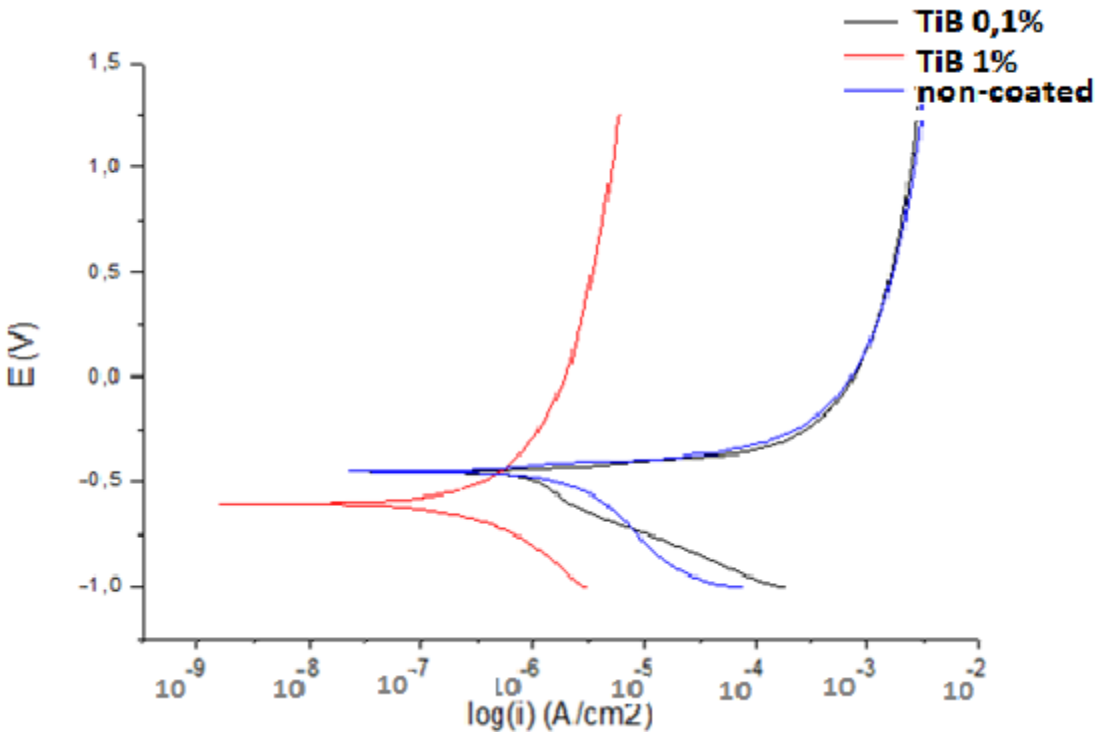


**Figure 13: Polarization curves of AA2024 in NaCl 0.05M for coated (TiB 1% and TiB 0,1%) and uncoated samples.**

Therefore, we conclude that silane films cured with a slightly high concentration of catalyst allowed the formation of better films and very low concentration do not have any effect on the silane network formation.

### 7.1.2 Surface analysis techniques

The silane film composed with MEMO/Bis-EGMP/TiB1% was analysed with SEM technique before being exposed to accelerated corrosion test. The analysis showed that the film had some cracks and was not well adhered on the metal surface. In Figure 16 there is a view from the top of the AA2024 coated surface and some cracks and bubbles are observed.

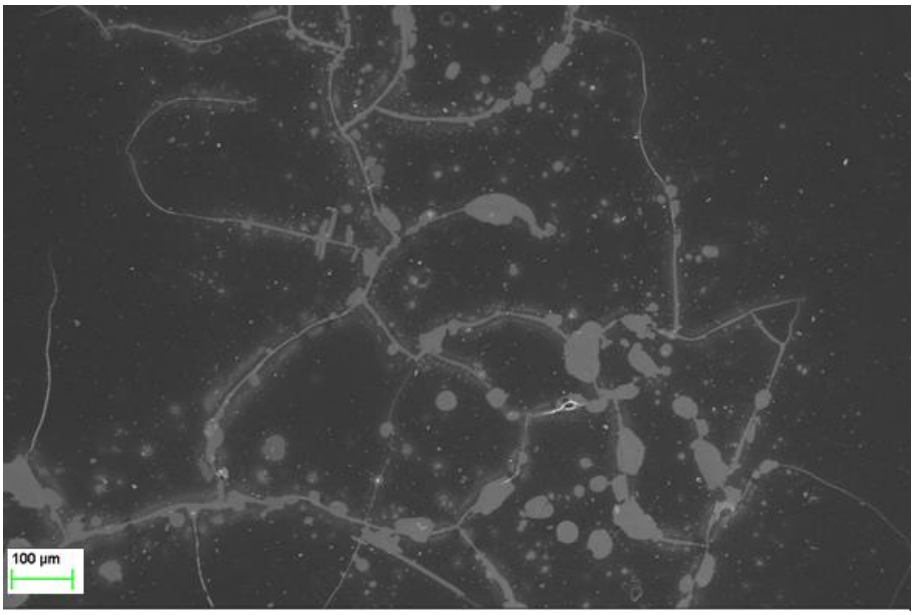


**Figure 14: SEM analysis from MEMO/Bis-EGMP/TiB1% silane film. Some cracks and bubbles are observed.**

On the other hand, in the Figure 17, we can see a detail of one zone where the silane film has been detached due to the extremely high brittle coating. It is possible to see some delaminated area and cracks of silane coating, and as aluminium substrate was polished, some scratches from this process are noted.


**Figure 15: Detail of the coating failed area. Some scratches from the polishing process can be noted on the aluminium surface.**

A lateral view of the same silane film showed in the Figure 17 can be seen in the Figure 18. It is possible to analyse the thickness of the film and how silane film interacts with aluminium surface. It is interesting to observe that not all the film is bonded to the surface; just some points are well jointed. The film thickness is about 55-65 µm, an extremely high thick for self-assembly monolayer formation. The micrographs explain why the corrosion performance of MEMO/Bis-EGMP/TiB1% (discussed in the next section) in NaCl solution and after the application of an epoxy topcoat was disastrous. This composition gave hybrid silane films extremely brittle and thick, therefore the coating obtained and the second layer deposited were not adhered.

We have to mention that SEM results were obtained after the accelerated corrosion test, because of this we performed the corrosion experiments with samples that not presented microscopic defects using optical microscope only.

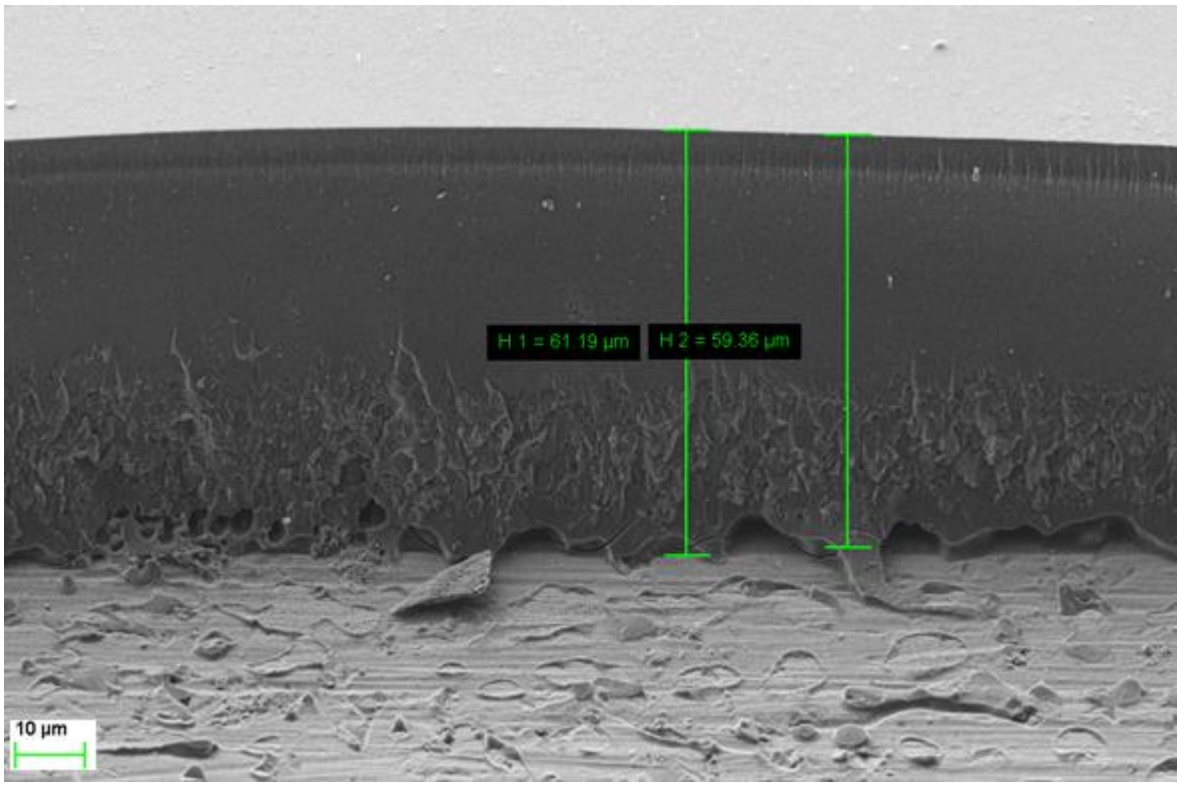


**Figure 16: Lateral view from the MEMO/Bis-EGMP/TiB1% coating, showing the thickness and poor adherence to the metal surface.**

### 7.1.3 Corrosion tests

The samples coated with MEMO-Bis EGMP-TiB did not show good results, as mentioned before. The samples composed by AA2024-silane-epoxy topcoat, called bilayer, suffered huge damage after only 3 days under accelerated corrosion condition (Figure 19). The film was completely detached from metal surface and several corrosion products appeared on the Al surface, due to the action of chlorine and oxygen species.

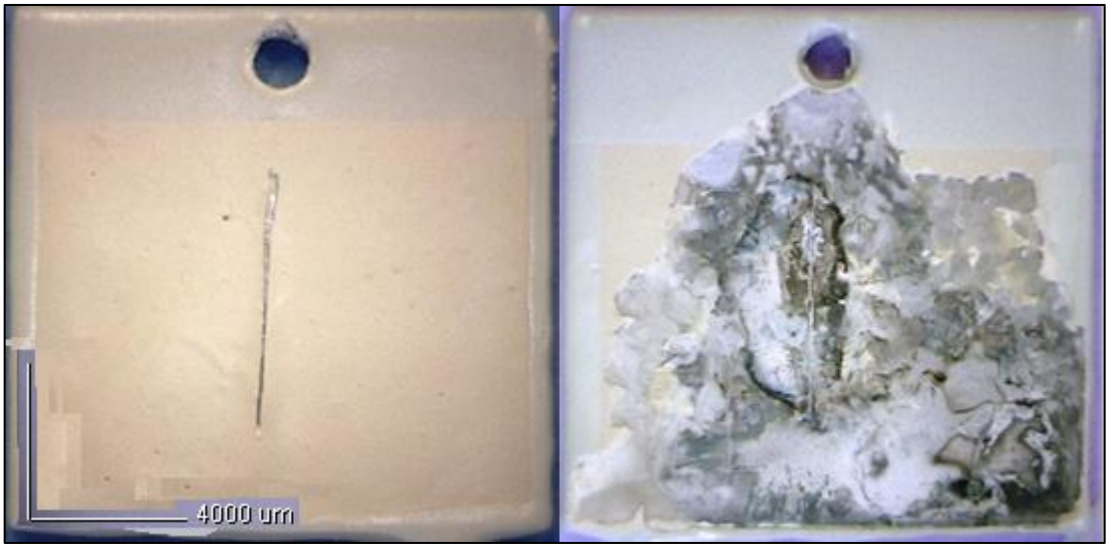


**Figure 17: Test panels composed by the bilayer system, showing the corrosion evolution. On the left side, the sample before the test and on the right side, after 3 days of immersion in NaCl 3.5% solution.**

Analysing Figure 20 it is possible to see that the silane coating did not have good adhesion with the substrate and neither with the epoxy topcoat. It was the main problem on this case, once the adhesion was not good; the electrolyte could diffuse between the layers and reaches the substrate causing severe aluminium corrosion.

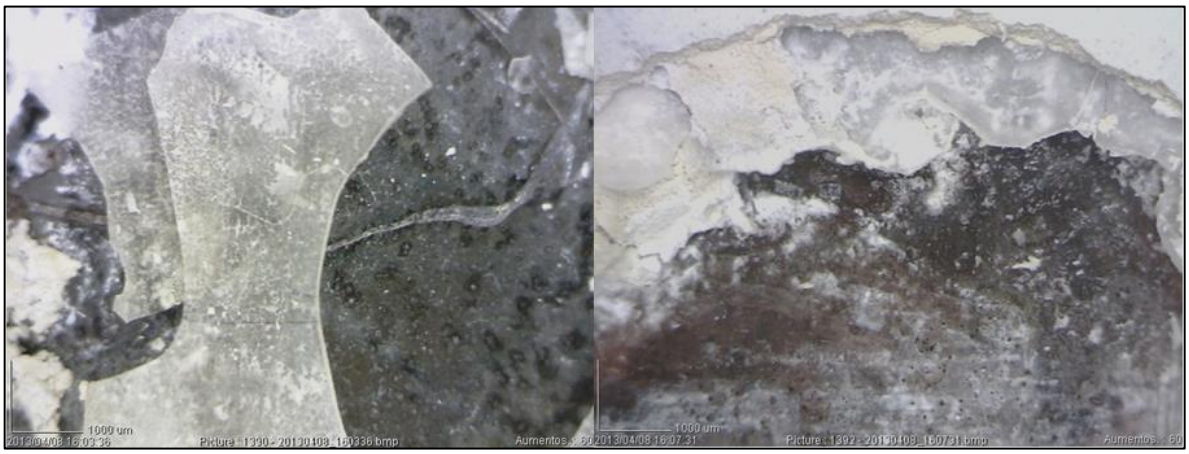

**Figure 18: On the right: delaminated silane (free of epoxy topcoat). On the left: separation between silane and epoxy topcoat.**

The results presented in this section contrast to that obtained with the polarization curves showed in the section 7.1.1. However, here the corrosion medium is more aggressive than that used in the polarization study, NaCl 3,5% compared to 0,05M, respectively. Additionally, results from accelerated corrosion assays are more representative than polarization analysis due to the larger area from the former compared to the later. Therefore, we conclude that the area chose in the polarization analysis was not representative of all the silane coating and another polarization analysis after three days of immersion would gave the same results of the accelerated corrosion assays, despite the lower NaCl concentration of the polarization solution.

## 7.2 Part B: Study of TEOS/ATMP/GPTMS system

### 7.2.1 Accelerated Corrosion Tests

At this step of the investigation, the behaviour of samples coated with TEOS/ATMP/GPTMS composition will be studied. Samples were exposed to a corrosion environment where the level of salt achieves 3,5%, as explained in the previous chapter. The samples were analysed under qualitative analysis (optical microscope and visual observation), adherence test (quantitative) and calculation of corroded affected area (quantitative) using ASTM D1654–05 standard methods. Additionally, some SEM micrographs were taken from the samples before and after panels extraction from the corrosion medium.

The samples were analysed weekly using the optical microscope and visual observation. The study persisted for 45 days. The samples covered only with epoxy, called monolayer, did not resist to the corrosion atmosphere more than 30 days, showing several blistering close to the scratch done on the coating surface, accordingly to the ASTM method. On the other hand, the samples treated with TEOS/ATMP/GPTMS had a good resistance under this environment, resisting until 45 days, and with none blistering formation. Corrosion products were only observed on the scratch.

On the Figures 21 and 22 the temporal evolution of the corrosion attack can be observed. Figure 21 shows the evolution of corrosion attack on surfaces covered with epoxy (monolayer, i.e. without silane intermediate layer). Figure 22 shows the same evolution with the bilayer system (silane+epoxy topcoat).

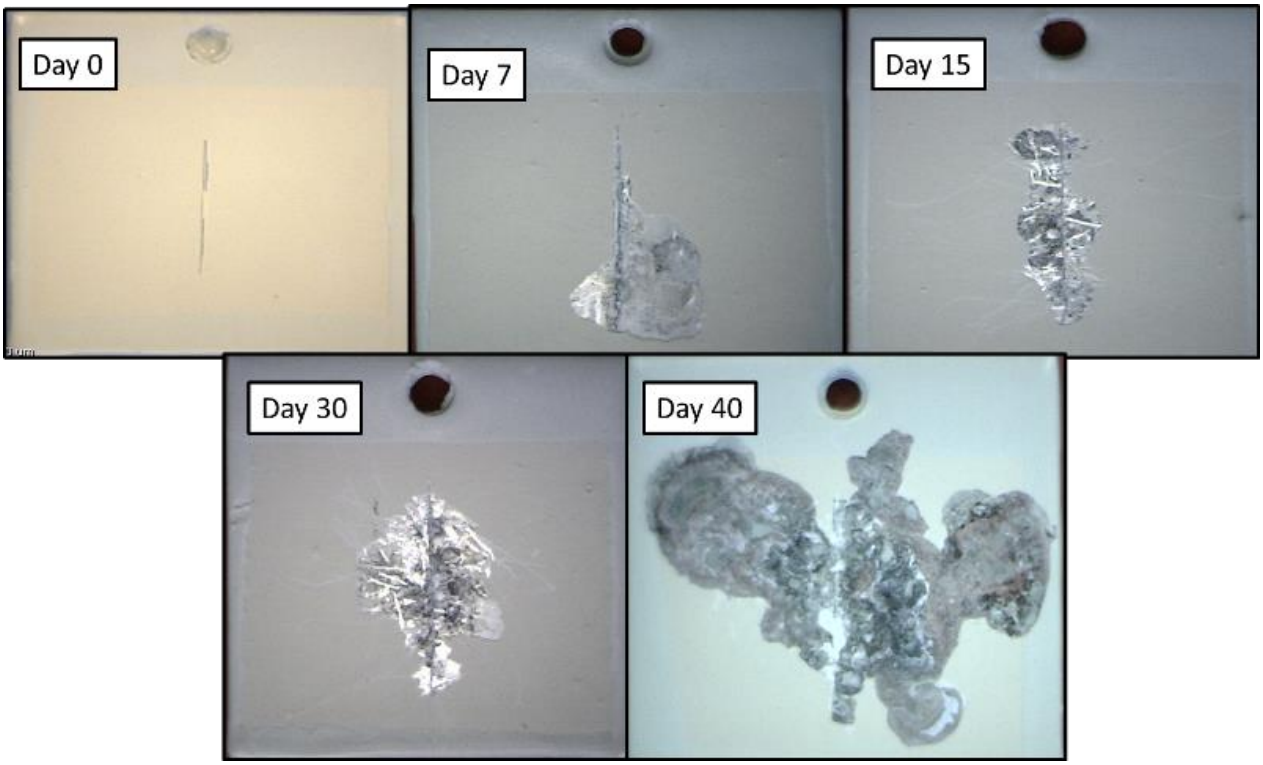


**Figure 19: Temporal evolution of corrosion on AA2024-T3 covered with painting, without silane application. Magnification: 15x.**

As we can see in the Figure 21, some coating delamination is observed with only seven days. The slightly spherical form of the corrosion progress from the scratch is a clear indication of blister formation under the coating and its propagation for all the aluminium surface after 40 days.

On the other hand, observing Figure 22 it is possible to notice that the silane has worked efficiently as an electrolyte barrier and adhesion promoter over the surface. The corrosion attack observed is just on the scratch and the propagation was avoided thanks to the well adhered silane layer with both the metal and the epoxy topcoat. The samples had resisted much more until 45 days after the test starts.

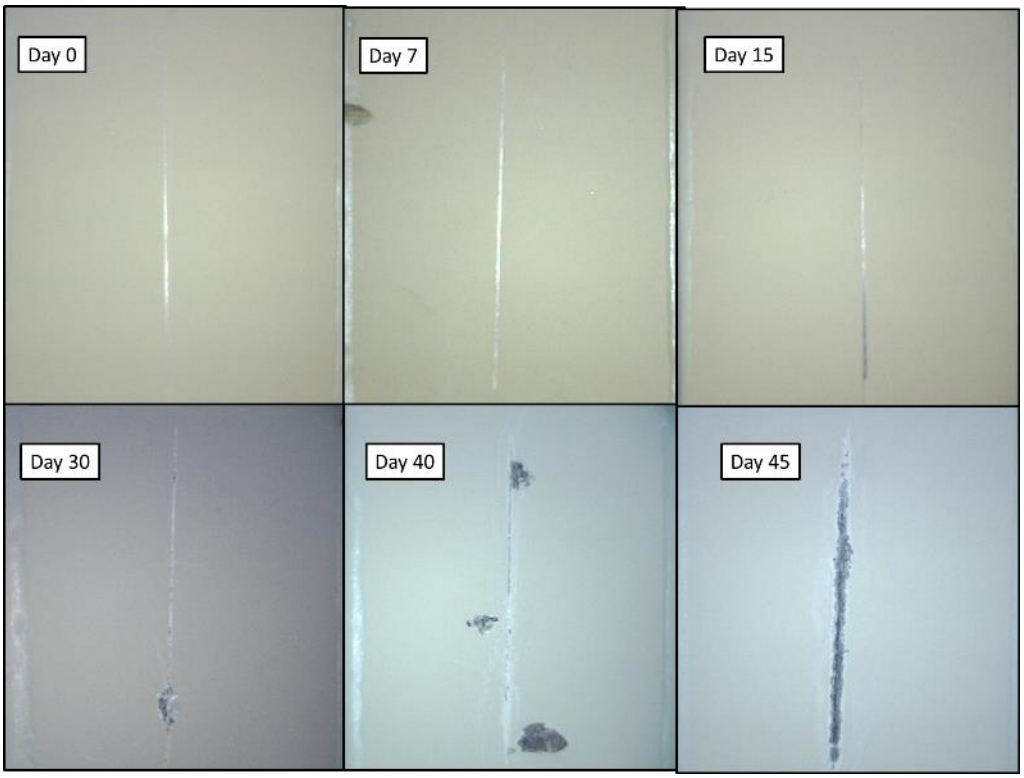


**Figure 20: Temporal evolution of corrosion on AA2024-T3 covered with silane and painting. Magnification: 15x.**

As explained above, the corrosion was generalized on samples without hybrid silane system. After 40 days, the entire sample was with bubbles and the painting was not resisting anymore, under the paint layer the aluminium was totally corroded. However, silane system and the bilayer protection were very efficient, the adherence was much better and the corrosion just appeared near the scratched area.

Figure 23 shows the corroded area near the scratch on a sample covered with silane. It is important to note that the cover layer is well adhered just beside the corroded area, no bubbles signs are noticed over the cover layer.

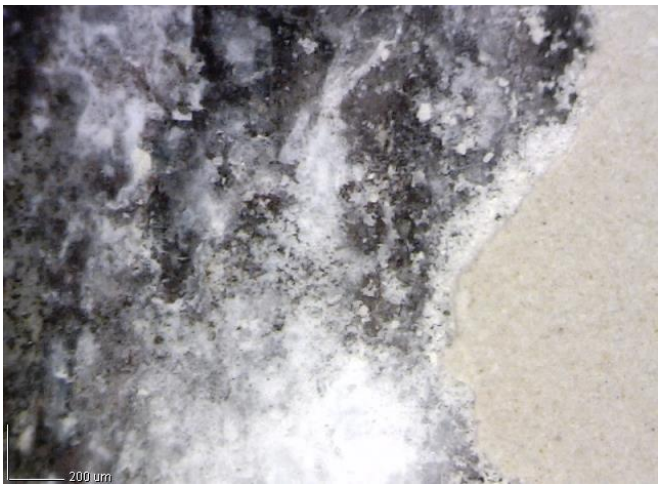


**Figure 21: Detail of zone between the scratch on the coating and the coating layer. The coating remains adhered even after 45 days. Magnification: 210x.**

Observing the results for adherence and failure area it is even clear the efficiency of the silane coat applied before the application of the epoxy layer (bilayer system protection). During the first 15 days, the samples covered with silane did not show any failure under this test. However, since the first 7 days, the samples without silane coating (monolayer) had some problems in adherence tests and affected areas because of the rapid corrosion evolution with the electrolyte penetration.

Figure 24 shows in the evolution of the failure at scribe in a graphic comparing the monolayer (Painting) and the bilayer system (Silane+painting). It is easy to notice how the silane protection is helpful to avoid damages, showing no failure at scribe until 30 days, whereas monolayer system has failure since the initial immersion time (5-7 days).

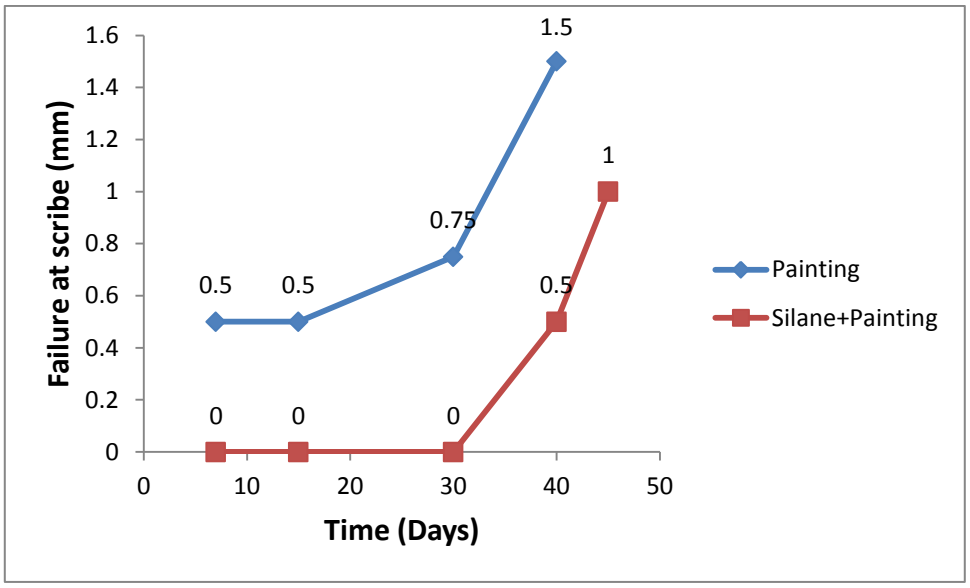


**Figure 22: Evolution of failure at scribe**

Analysing Figure 25, it is possible to notice the temporal evolution of corrosion affected areas in the both samples. At the end of 45 days, just 5% of the sample area covered with silane was attacked by corrosion. On the opposite, the samples without silane treatment had more than 50% corroded at the end of 40 days.

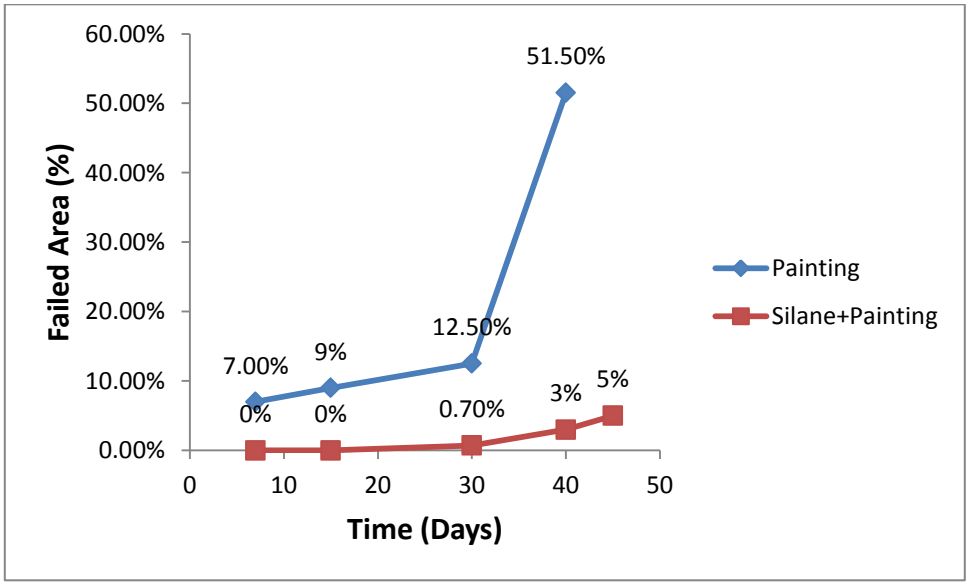


**Figure 23: Evolution of failed unscribed areas.**

With these information it is possible to rate the specimens tested accordingly to the Table 2 showed on anterior chapters. The rating for failure at scribe and rating of unscribed area is seen in Table 4. In both tests, the specimens coated with silane and painting had better rate. According to the ASTM D1654–05 statements, high rates are related to less attack and in the opposite, low rates are related to several attack.

**Table 4: Specimens Rating**

| Ratings | | | |
|---|---|---|---|
| Failure at scribe | | Unscribed Area | |
| Painting | Epoxy+Silane | Painting | Epoxy+Silane |
| 7 | 8 | 2 | 7 |

Due to the interesting results obtained from hybrid silane systems for AA2024 protection, we decided perform some SEM analysis and EDX in order to see the corrosion product morphology and composition.

The three painted panels tried to this study were that showed in the Figure 21 (Day 0), Figure 21 (Day 40) and Figure 22 (Day 45). The three panels were cut in half with a saw and polished with a mechanical polishing before the SEM inspection. The main aims were to see the interface between the epoxy topcoat and the metal substrate with or without silane deposition and the surface corrosion products obtained.

In the Figure 26, we see the poor adherence of the epoxy topcoat with the AA2024 substrate (monolayer system). The coating has an important separation from the metal in some zones. The Figure 26 (right) shows a detail of the zone pointed in the left micrograph, here we also observe that the bad corrosion results obtained for this sample is caused in part by its poor adherence and its high porosity. The thickness of the epoxy top coat is around 68-70 μm.

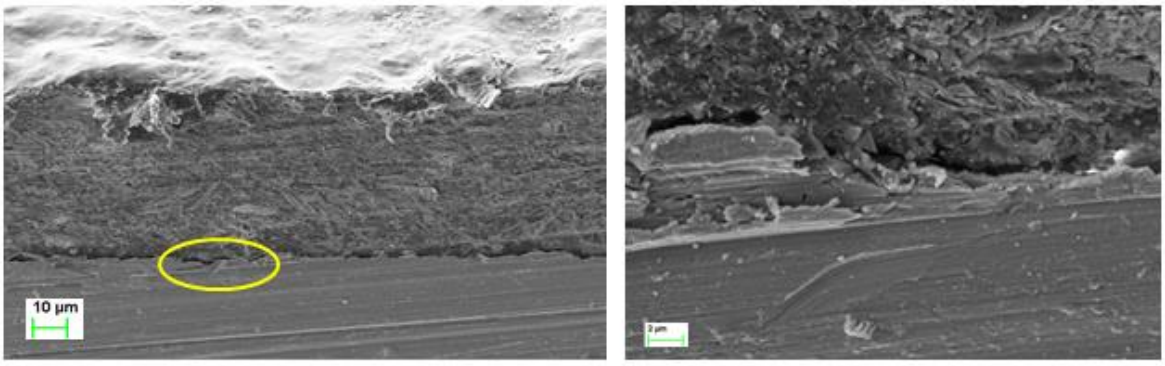


**Figure 26: AA2024 test panel covered with epoxy topcoat only (initial sample, without immersion on NaCl solution). On left: low magnification (1000X) and on right: high magnification (10kX).**

In the Figure 27 we can appreciate the micrograph for the bilayer system protection, composed by the hybrid silane and the epoxy topcoat. As we can see, after 45 days of immersion in aggressive solution, the epoxy maintain well adhered and we did not observed the same interface separation observed for the monolayer system, explained above. We attribute this good result to the silane layer, which acts as both metal adherence promoter (with covalent bonded Si-O-Al and P-O-Al linkages) and topcoat adherence promoter.

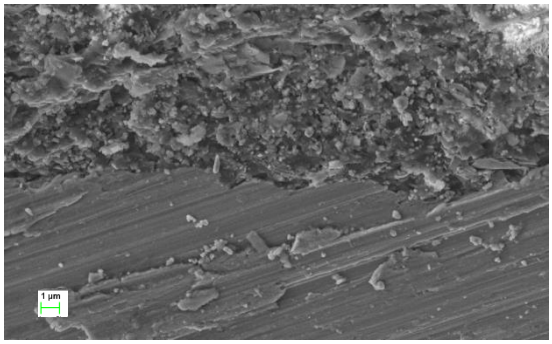

**Figure 27: AA2024 test panel covered with hybrid silane film and the epoxy topcoat only (after 45 days of immersion in NaCl solution). Magnification: 10kX.**

On the other hand, corrosion appeared discretely only in the longitudinal scratch done before start the accelerated corrosion tests (as we can see in the Figure 22, Day 45), according to the ASTM D1654-05. Figure 28 shows the corrosion product

obtained in the scratch, which is mainly composed by $Al_2O_3$ precipitates, as corroborated by EDX analysis (spectrum not showed).

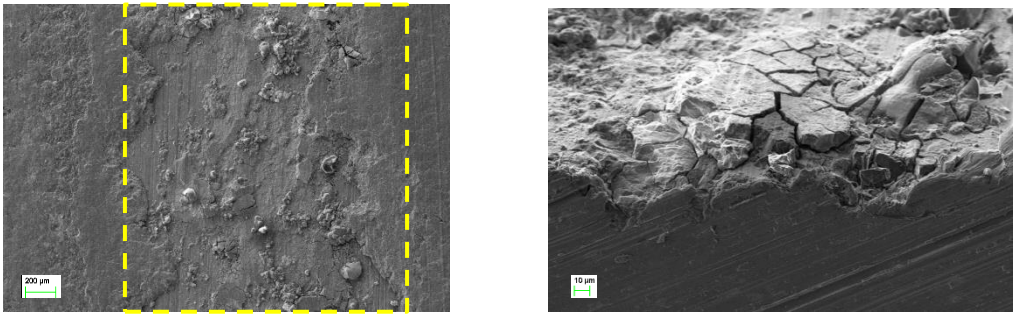

**Figure 28: Corrosion products formed only in the scratch zone of the AA2024 covered with silane and epoxy topcoat. On left: dashed line represents the scratch limits on coating (Magnification: 100 X). On right: lateral view of corrosion products on the scratch (Magnification: 1000 X).**

Finally, when we analyse in detail the different zones of corrosion products formed at the surface of aluminium alloy (Figure 29), we can appreciate different morphologies corresponding to different oxides nature (Figure 30-32).

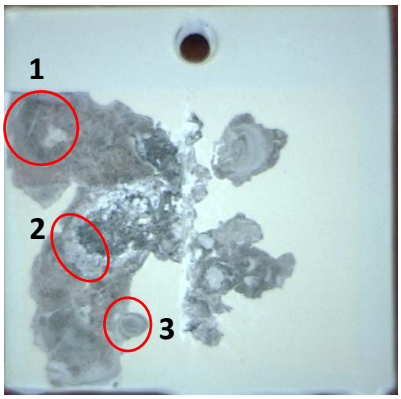


**Figure 24: Test panel coated with epoxy topcoat after 40 days of immersion in NaCl 3.5% solution and showing the main corrosion area analysed by SEM.**

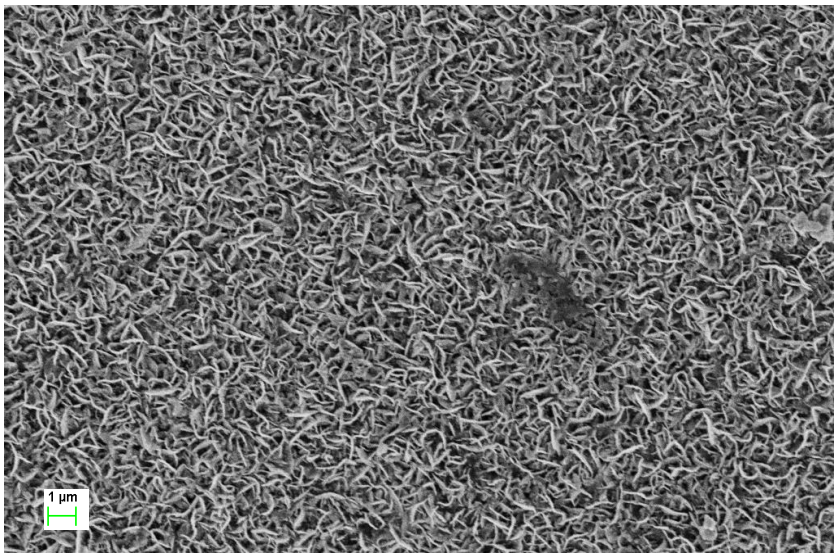


**Figure 30: SEM micrographs of the zone 1 showed in the Figure 29 (magnification: 10 KX).**

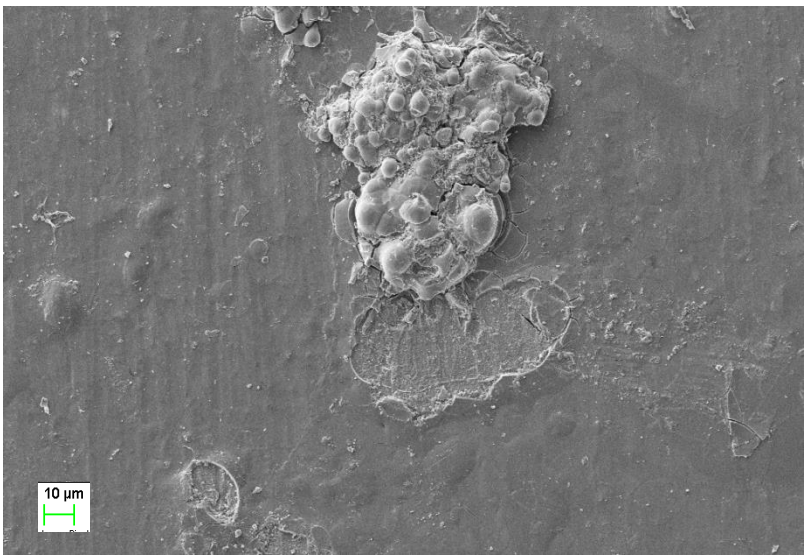


**Figure 31: SEM micrographs of the zone 2 showed in the Figure 29 (magnification: 1000 X).**

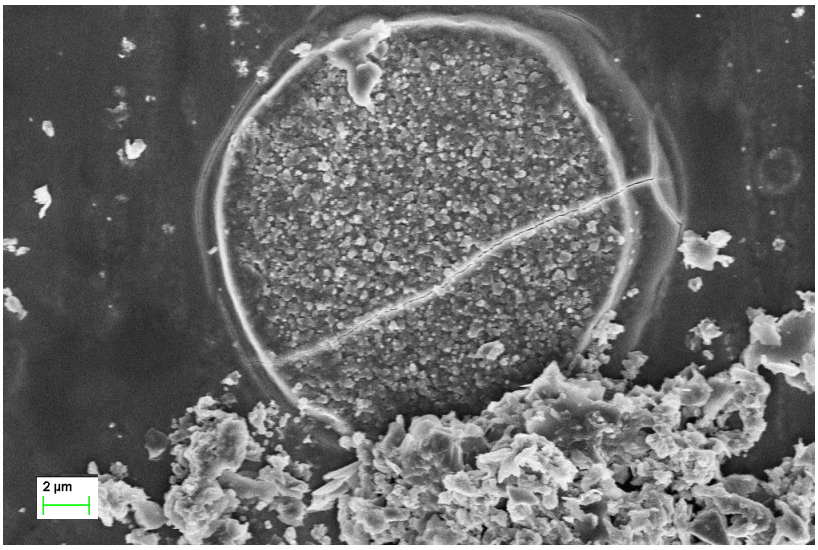


**Figure 32: SEM micrographs of the zone 2 showed in the Figure 29 (magnification: 8400X).**

According to EDX analysis, the corrosion product showed in the Figure 30 is mainly iron oxides from the aluminium alloy composition, whereas the bigger structures observed as white oxides in the Figure 31, corresponds to $Al_2O_3$. Finally, the composition found for the precipitates formed in the zone 3 (Figure 32) are mainly the $CuCl_2$ derived from the high concentration of copper in the AA2024 composition.

Therefore, we conclude that the corrosion products formed when the substrate are not coated with silane derivative are more aggressive than we have the silane film. This is one of the reasons why the coating suffer a rapid delamination, i.e. due to the rapid progress of corrosion products under the coating.

### 7.2.2 Pull-off adherence test

The specimens were tested accordingly to ISO 4624:2002– “Paints and varnishes: Pull-off test for adhesion”, as explained in Experimental section. Figure 33 shows the evolution of adherence during the corrosion accelerated test. Before being exposed to the test, the samples coated with silane had better

adherence, and after 30 days as well. The samples coated only with epoxy did not resist to corrosion after 40 days, and the breaking strength of pull-off test showed almost zero adherences.

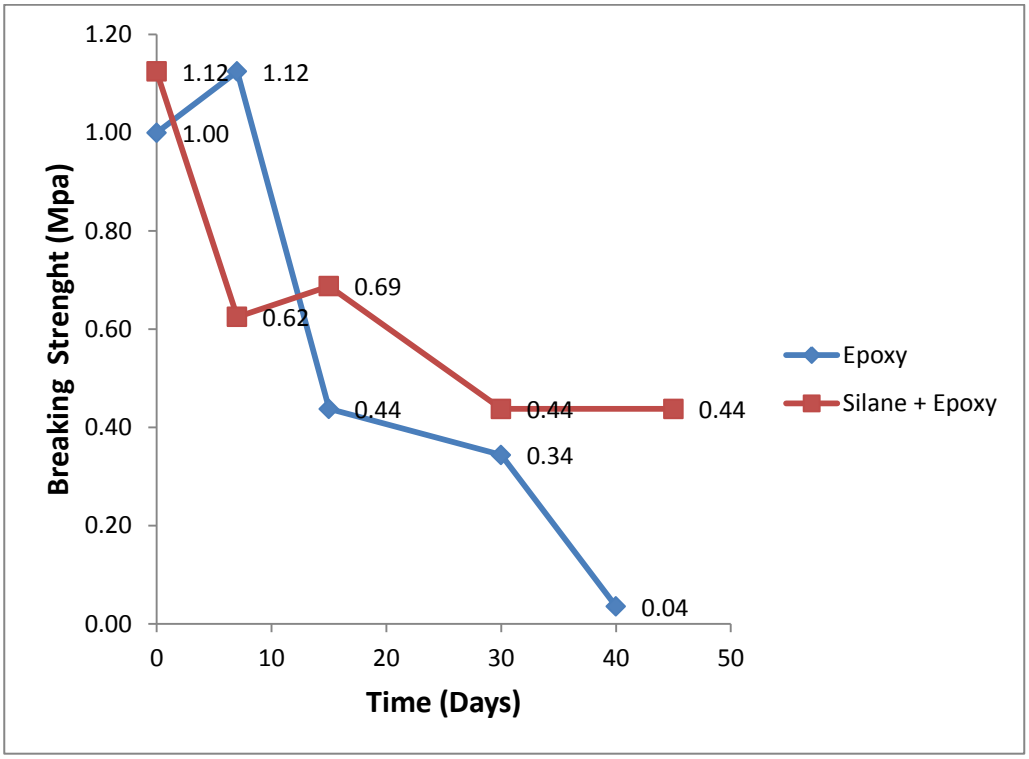


**Figure 33: Evolution of breaking strength - Pull-off test**

Table 5 shows the nature of breaking for each point of the graphic showed in the Figure 33.

**Table 5: Nature of breaking during pull-off test according to ISO 4624.**

| Epoxy | | | Silane + Epoxy | | |
|---|---|---|---|---|---|
| Time (Days) | Breaking Force KgF | Nature | Time (Days) | Breaking Force Kgf | Nature |
| 0 | 32 | Y | 0 | 36 | B and -Y |
| 7 | 18 | -Y | 7 | 20 | Y |
| 15 | 36 | AB | 15 | 22 | -Y |
| 30 | 14 | -Y | 30 | 14 | -Y and A/B |
| 40 | 11 | Y | 45 | 14 | -Y |

This table shows that the highest point for breaking strength of epoxy coating is the one where the nature was Y. This represents cohesive failure of adhesive. Almost all the Silane+Epoxy coating presented the same nature, however, the breaking strength is clearly higher compared to the monolayer composition.

With the time exposure, Epoxy+Silane coating keeps with higher adherence, as showed on the Figure 26. After 40 days the adherence for this coat is higher than the monolayer protection system. It is also important to remember that after 40 days, the samples painted with epoxy coating, did not resist to the corrosion attack. Therefore, we can say that the breaking strength is zero for the monolayer compared to 0,44 MPa for the same substrate coated with an intermediate layer of silanes.

The samples coated with epoxy had a sharp decrease on adherence meanwhile the silane+epoxy coated samples had one gradually decrease, tending to stabilize.

# 8. Conclusions

Part A: Study of MEMO/Bis-EGMP/TiB system

(i) The use TiB 1% on silane coat was not efficient on forming the silane layer, due to the extremely high brittleness and thickness.

(ii) The use of 0,1% of TiB was not enough for catalysing the reaction for the coating formation. The layer obtained was cracked and did not offer protection against corrosion.

(iii) Microstructures analysis on the covered samples showed that some microcracks caused problems of adherence between the silane coat and the aluminium surface. This micro defects represent a problem during corrosion tests, as the electrolyte could diffuse across the layer and rapidly reach the metal surface.

Part B: Study of TEOS/ATMP/GPTMS system

(i) The system showed a high efficiency on protecting the aluminium substrate. The samples covered with silane and epoxy topcoat had better protection results than the monolayer (epoxy coating alone) in NaCl 3.5 aggressive medium.

(ii) The silane improves the coating adherence, as observed by SEM and by pull-off tests.

Therefore, TEOS/ATMP/GPTMS system represents a new alternative to the current AA2024 mechanisms of protection mentioned in the Stat of Art.

# 9. References

ÁLVAREZ, P. *et al.* The electrochemical behaviour of sol–gel hybrid coatings applied on AA2024-T3 alloy: Effect of the metallic surface treatment. **Progress in Organic Coatings**, v. 69, n. 2, p. 175-183, 2010.

DALMORO, V. **REVESTIMENTOS A BASE DE TEOS COM INCORPORAÇÃO DE ÁCIDOS FOSFÔNICOS COMO PRÉ-TRATAMENTO PARA LIGAS DE ALUMÍNIO**. [s.l.] UFRGS, 2009.

DALMORO, V.; *et al.* Corrosion behavior of AA2024-T3 alloy treated with phosphonate-containing TEOS. **Journal of Solid State Electrochemistry**, v. 16, n. 1, p. 403-414, 6 abr. 2011.

DIETRICH G. ALTENPOHL. **Aluminum: Technology, Applications and Environment. A profile of a modern metal.** 6º. ed. 1998

DURÁN, A. *et al.* Protection and surface modification of metals with sol–gel coatings. **International Materials Reviews**, v. 52, n. 3, p. 175-192, 2007.

JOSHUA DU, Y. *et al.* Inorganic/organic hybrid coatings for aircraft aluminum alloy substrates. **Progress in Organic Coatings**, v. 41, n. 4, p. 226-232, 2001.

KANNAN, A. G.; *et al.*Synthesis and characterization of methacrylate phospho-silicate hybrid for thin film applications. **Polymer**, v. 48, n. 24, p. 7078-7086, 2007.

LABJAR, N. *et al.* Corrosion inhibition of carbon steel and antibacterial properties of aminotris-(methylenephosphonic) acid. **Materials Chemistry and Physics**, v. 119, n. 1-2, p. 330-336, 2010.

LIU, F. *et al.* Optimizations of inhibitors compounding and applied conditions in simulated circulating cooling water system. **Desalination**, v. 313, p. 18-27, 2013.

LIU, Y. *et al.* Corrosion resistance properties of organic–inorganic hybrid coatings on 2024 aluminum alloy. **Applied Surface Science**, v. 246, n. 1-3, p. 82-89, 2005.

MRAD, M. *et al.* Deposition of hybrid 3-GPTMS's film on AA2024-T3: Dependence of film morphology and protectiveness performance on coating conditions. **Progress in Organic Coatings**, v. 73, n. 2-3, p. 264-271, 2012.

NATARAJAN, R.; *et al.* Contributed papers Inhibition by phosphonic acids – an overview. v. 44, n. 4, p. 248-259, 1997.

PERES, R. S. **PROPRIEDADES ANTICORRROSIVAS DE CAMADAS DE CONVERSÃO À BASE DE TANINOS COMO PRÉ-TRATAMENTO PARA O AÇO CARBONO 1020**. [s.l.] UFRGS, 2010.

RAPS, D. *et al.* Electrochemical study of inhibitor-containing organic–inorganic hybrid coatings on AA2024. **Corrosion Science**, v. 51, n. 5, p. 1012-1021, 2009.

ROSERO-NAVARRO, N. C. *et al.* Improved corrosion resistance of AA2024 alloys through hybrid organic–inorganic sol–gel coatings produced from sols with controlled polymerisation. **Surface and Coatings Technology**, v. 203, n. 13, p. 1897-1903, 2009.

SHAO, M. *et al.* A study on pitting corrosion of aluminum alloy 2024-T3 by scanning microreference electrode technique. **Materials Science and Engineering: A**, v. 344, n. 1-2, p. 323-327, 2003.

THI XUAN HANG, T. *et al.* Corrosion protection of carbon steel by an epoxy resin containing organically modified clay. **Surface and Coatings Technology**, v. 201, n. 16-17, p. 7408-7415, 2007.

WANG, D.; *et al*. Sol–gel coatings on metals for corrosion protection. **Progress in Organic Coatings**, v. 64, n. 4, p. 327-338, 2009.

WITTMAR, A. *et al.* Hybrid sol–gel coatings doped with transition metal ions for the protection of AA 2024-T3. **Journal of Sol-Gel Science and Technology**, v. 61, n. 3, p. 600-612, 2012.

WU, K. H. *et al.* Thermal stability and corrosion resistance of polysiloxane coatings on 2024-T3 and 6061-T6 aluminum alloy. **Surface and Coatings Technology**, v. 201, n. 12, p. 5782-5788, 2007.

ZHANG, W.;*et al.* Transitions between pitting and intergranular corrosion in AA2024. **Electrochimica Acta**, v. 48, n. 9, p. 1193-1210, 2003.

ZHANG, X. *et al.* Structural characterization of sol–gel composites using TEOS/MEMO as precursors. **Surface and Coatings Technology**, v. 201, n. 12, p. 6051-6058, 2007.

ZHELUDKEVICH, M. L. *et al.* Nanostructured sol–gel coatings doped with cerium nitrate as pre-treatments for AA2024-T3. **Electrochimica Acta**, v. 51, n. 2, p. 208-217, 2005.

ZHELUDKEVICH, M. L. *et al.* Corrosion protective properties of nanostructured sol–gel hybrid coatings to AA2024-T3. **Surface and Coatings Technology**, v. 200, n. 9, p. 3084-3094, 2006.

ZHENG, S.; *et al.* Inorganic – organic sol gel hybrid coatings for corrosion protection of metals. p. 174-187, 2010.

# 10. Acknowledgments

The IMEM's Group investigation has been supported by MICINN and FEDER funds (MAT2009-09138 and MAT2012-34498) and by the DIUE of the Generalitat de Catalunya (contract number 2009SGR925).

C. Velasques Ugarteche acknowledges the fellowship provided by the Brazilian Government Agency CNPq for the financial support of this project as part of "Ciências sem Fronteiras" exchange program.